Wednesday afternoon excursion in Sidmouth with a visit to the Norman Lockyer Observatory to enjoy a rich program of fun-fair demonstrations and shows (bottom left: D. Webb and S. Strawbridge) and the scenic walk down the coastal path.

Part 4. Impact of Solar wind, Structures and Radiation on Ionospheres, Atmospheres

Space Weather of the Heliosphere: Processes and Forecasts
Proceedings IAU Symposium No. 335, 2017
C. Foullon & O.E. Malandraki, eds.

doi:10.1017/S174392131700919X

Thermospheric Dynamics in Quiet and Disturbed Conditions

Aziza Bounhir[1,2], Zouhair Benkhaldoun[1], Jonathan J. Makela[3], Mohamed Kaab[1], Brian Harding[3], Daniel J. Fisher[3], Amine Lagheryeb[1], Malki Khalifa[1], Khaoula Elbouyahyaoui[1], Mohamed Lazrek[1] and Ahmed Daassou[1]

[1]High Energy Physics and Astrophysics Laboratory, Oukaimeden Observatory, Cadi Ayyad University, Marrakech, Morocco
[2]High Energy Physics and Astrophysics Laboratory, Faculty of Sciences and Techniques, Marrakech, Morocco
[3]Department of Electrical and Computer Engineering, University of Illinois at Urbana-Champaign, Illinois 61801, USA, Urbana, IL, United States

Abstract. This paper presents the thermospheric winds and temperature properties measured with a Fabry-Pérot interferometer (FPI) over Oukaimeden observatory ($31.2°N$, $7.8°W$, $22.8°N$ magnetic) in Morocco. After Three years of successful functioning from 2014 to 2017, we can address the seasonal behavior of the temperature and the winds (vertical, zonal and meridional). The dependence of the thermospheric winds and temperature on the solar cycle is also presented. The day-to-day variations of the quiet time wind pattern exhibits the importance of other type of waves superposed to the main diurnal tides. The storm time wind and temperature exhibits also a variety of ways to react to the storm. However, there is seasonal effect to the storm that will be illustrated in this paper. The signature of the MTM phenomenon is also present in the winds and temperature in geomagnetically quiet and disturbed nights. The occurrence of this phenomenon over the studied area is also addressed.

Keywords. Ionosphere, Thermosphere, Geomagnetic storm, Fabry-Perrot Interferometer.

1. Introduction

Space weather is defined as the conditions on the Sun and the near-Earth space that can influence the performances of space based and terrestrial technological instruments and endanger human health. The thermosphere/ionosphere system plays a dramatic role as a vehicle of space weather events. After a solar flare or a geomagnetic storm, the ionospheric density changes and affects the ground-to-ground and ground-to-satellite signals. Navigation and communication satellites links can be degraded or lost. Currents can be induced in power grids causing failure and satellite assets can be damaged by increased energetic particle radiation during geomagnetic storms.

One of the most challenging problems in space weather is the forecasting of the ionosphere as it is related to most of space weather events. A crucial step towards the forecasting of the ionosphere is the thorough understanding of the coupling between the charged and neutral particles in the presence of a magnetic field. Drag forces between the charged and neutral gases produce complex electrodynamic interactions. Variations in the neutral wind can drive a complex system of ionospheric currents and electric fields, which profoundly influence the structure and composition of the ionosphere.

In this paper, we will present the thermospheric measurements of a Fabry-Perrot interferometer (FPI) over the Oukaimeden observatory ($31.206°N$, $7.866°W$, $22.84°N$ magnetic). The FPI (Makela & Miller 2011, Harding *et al.* 2014) measures the thermospheric

wind and temperature by observing the 630-nm airglow generated by the dissociative recombination of O_2^+ which takes place at an average altitude of 250 km approximately (Link & Cogger 1988). The data from The FPI over Oukaimeden can be used to test and improve the existing thermospheric models and help improve our understanding of actual physics behind the atmosphere. The seasonal variability of the zonal and meridional winds and the temperature are presented along with the dependence on solar cycle. We will address the variability for geomagnetically disturbed and quiet conditions. During a geomagnetic storm, the thermospheric winds and temperature depart from their quiet time behavior and exhibit multiple ways to react to the storm. Finally, the seasonal effect of the storm will be illustrated.

2. Climatology of the winds and quiet time patterns

The basic climatology of the winds is well documented in Kaab *et al.* (2017). To build the climatology they adopted the method developed by Fisher *et al.* (2015). The data were over-averaged to compare with existing thermospheric models that has low spatial resolutions. In this case the climatology was compared with HWM14 empirical model (Drob *et al.* 2015). Figure 1 shows a sample of very quiet time wind data with sum-Kp index less than 6. The south (green) and north (red) look of the meridional winds are illustrated as well as the east (yellow) and west (purple) components of the zonal winds. We can clearly notice the superposition of many waves to the main diurnal tides. Small harmonics of tides and gravity waves contribute to the habitual flow of the winds. In Figure 1, the zonal components of the winds have most of the time the same magnitude. This is not the case of the equatorward flow of the meridional winds. Between 00 and 04 UT, the northern component has a larger magnitude than the southern one; of about 50 $m.s^{-1}$ for Figure 1 (a) and 90 $m.s^{-1}$ for Figure 1 (c). Given the geographical position of Oukaimeden Observatory at about 31° North, the northern component is certainly more sensitive to equatorward flows and has a larger magnitude. The southern component on the other hand is more sensitive to northward flows originating from regions of lower latitudes or from the equator. The northward surge of the Midnight Temperature Maximum (MTM) phenomenon is present in the wind flow between 02 and 04 UT.

The day-night differential solar heating drives the thermospheric wind dynamics. The eastward zonal wind combined with upward propagating tidal meridional winds and in situ tidal create a large-scale structure (Akmaev *et al.* 2010) converging onto the geographic equator. The convergence of the thermospheric tides creates an equatorial pressure bulge which bifurcates and propagates to higher latitudes in both hemispheres. The MTM peak formed by hydrostatic expansion migrates toward both polar regions and reverses the direction of the meridional component of the thermospheric wind from its normally equatorward flow to poleward flow. This northward surge transfers the F region plasma along magnetic field lines to lower altitudes, thus generating an increase in the 630.0 nm nightglow emission which creates the brightness wave and the descent of the F-region plasma, termed 'midnight collapse'.

The multiple forcing of the sun upon the Earth make it a gigantic electrical machine with many currents flowing in multiple places and make it also a gigantic nonlinear resonator because Earth atmosphere displays a wave-like structure on a global scale. Multiple forms of planetary waves, tides and gravity waves superpose on the Earth's atmosphere. Tidal waves (Chapman & Lindzen 1970, Forbes & Garrett 1979) are primarily formed by the regular differential heating of the atmosphere such as the day-night and seasonal differential heating. We can mainly distinguish migrating and

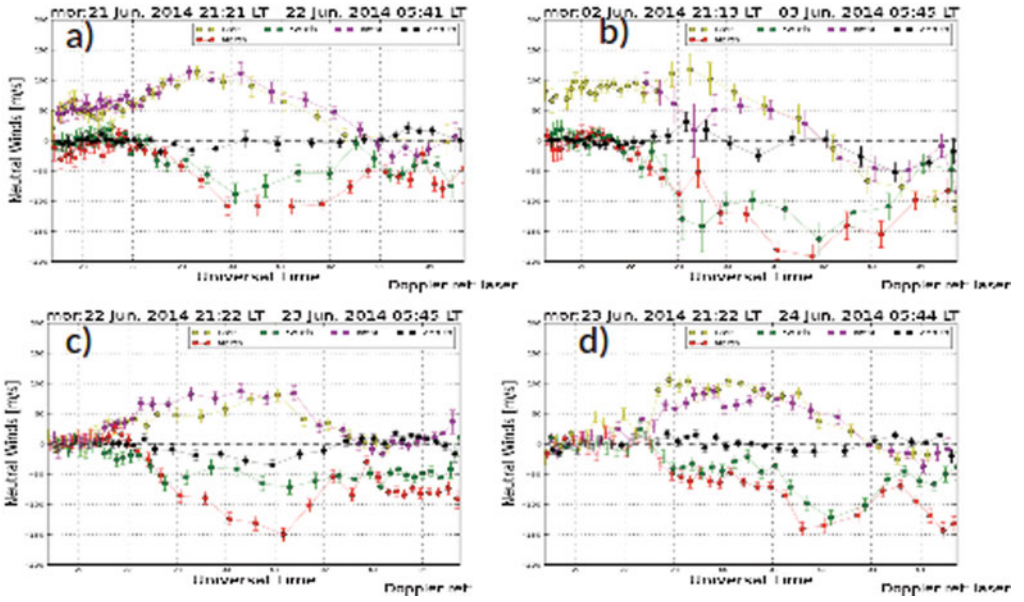

Figure 1. Very quiet time thermospheric winds dynamics. Data from Fabry-Perrot interferometer using Doppler shift and broadening of the 630 nm airglow.

non-migrating tides and stationary and upward propagating tides. Westward-migrating tidal modes dominate the upper-atmosphere response. Upward propagating waves in general can transport a huge amount of energy from low to high altitudes. As their wind amplitude grow with increasing altitude, they reach a point where they break and strong dissipation of energy occurs in the thermosphere. The change in thermospheric dynamics and properties affects immediately the composition, density and electrodynamics of the ionosphere. Therefore, modeling and observations of these type of waves are needed in order to monitor and predict changes in the ionosphere (Hagan & Forbes 2002).

In Figure 1 (d), we can notice an additional equatorward surge felt only by the northern component of the wind between 03 and 04 UT. In Figure 1 (b) between 23 and 00 UT superimposed to the wind general trend, a surge that have pushed the northern component towards the north, the southern component towards the south, the eastern component toward the east and the western component towards the west. This is a very interesting phenomenon occurring above the area under study and could be a signature of an upward propagating tides or a breaking gravity waves. This type of forcing mechanisms are mostly ignored in the thermospheric models. In is important to see that the vertical component of the wind is not negligible and can reach 30 to 50 $m.s^{-1}$ in very quiet time nights.

3. Seasonal variability

To address the seasonal variability, we have adopted the same method as for the climatology (Fisher *et al.* 2015) but averaged the data in 15 *mn* interval. The north and south look contribute to the meridional component of the wind and the east and west look contribute to the zonal one. Figure 2 illustrates the seasonal variability of the temperature (left), zonal winds (middle) and meridional winds, for the years 2014 (top), 2015 (middle) and 2016 (bottom). All the data have been considered regardless

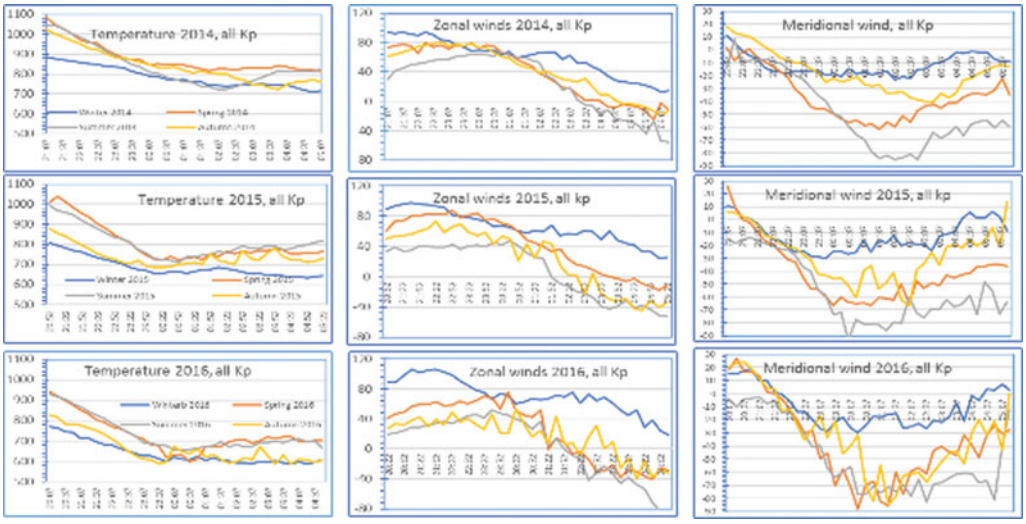

Figure 2. Seasonal behavior of the thermospheric temperature (left) and zonal (middle) and meridional (right) winds on a year-to-year basis.

of geomagnetic conditions. The contribution of all heating mechanisms is present. The temperature cools down during the night. In the early evening hours, the temperature decreases almost linearly with a slope depending on the season and the year. At around 23 to 00 UT, there is an inflexion point towards another regime where the temperature undergoes a series of increases and decreases around a constant value. These oscillations are mostly pronounced in Autumn months and in declining solar cycle. We can see in all years that the winter is the coolest and the spring the hottest along with the summer. 2014 summer temperature is particularly cold between 00 and 03 UT, even though 2014 is the maximum solar cycle. This could be due to the surprisingly geomagnetically very quiet summer.

The post-midnight oscillations are mainly caused by the Midnight Temperature Maximum (MTM) phenomenon. The heating caused by geomagnetic storms is also present in the temperature variations. Zonal winds are the strongest during winter time for all years. They are also eastward during the entire night. They abate in other seasons and reverse to westward direction in summer months. The time of reversal depend on the year. We can also notice small time scale variations especially in Autumn and spring 2016. Concerning the meridional winds, winter equatorward flow is the weakest and summer is the strongest for all years. The maximum equatorward flow shifts to later hours from spring to summer to autumn especially in 2014. Autumn and spring components are very dynamic in 2015 and 2016.

Vertical winds are illustrated in Figure 3 where we compare 2014 and 2015 seasons. We can clearly notice seasonal effect of the vertical winds. In winter time, the vertical winds are upward in the early evening hours with an average of 5 $m.s^{-1}$ and abates and reverse to downward direction before sunrise. In other seasons, the vertical winds are flowing downward in the early evening hours with an average of 5 $m.s^{-1}$ and upward before sunrise for summer, autumn and spring. We can clearly notice average seasonal values of, for example, 20 $m.s^{-1}$ in sometimes.

Large vertical wind observations have been difficult to reconcile with theory because they have an enormous impact on the dynamics, chemistry, and electrodynamics of the ionosphere/thermosphere system. Vertical gradients of composition, density, and

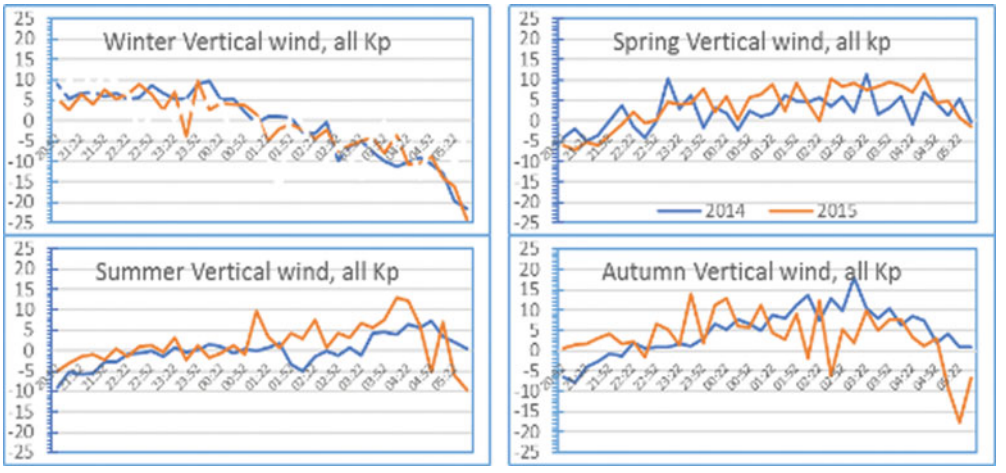

Figure 3. Seasonal behavior of the vertical winds related to 2014 and 2015 years.

temperature are larger than horizontal gradients, so even a small vertical wind causes large advective transport and adiabatic temperature changes. Vertical winds are supposed to be low of 1 $m.s^{-1}$ under hydrostatic balance of an atmosphere subject to diurnal heating (Smith *et al.* 1998), but localized source of heating and divergent horizontal flows can drive the divergent component of the vertical wind. However very high vertical winds lasting for long time seem not reasonable. (Makela & Miller 2011) reported large vertical winds lasting for several hours in many midlatitude places and concluded that these large apparent vertical winds must be an artifact of some type of contamination of non thermospheric origin. Harding (2017) developed a radiative transfer model which demonstrates that these measurements can be explained as an artifact due to the scattering of airglow light by tropospheric aerosol layer.

4. Variability with the solar cycle

To address the seasonal variability with the solar cycle, Figure 4 shows the evolution of 2014, 2015 and 2016 seasons related to thermospheric temperature, the zonal and meridional winds. We can notice that the zonal winter wind does not depend on solar cycle. In the other seasons, the magnitude of the zonal wind decreases with declining solar cycle. In summer months, the reversal time from eastward to westward direction seems to shift to earlier hours with the declining solar cycle. For autumn and spring months, zonal winds abate before sunrise in 2014 and reverse to westward direction in 2015 and 2016 months. The time of reversal depends on solar cycle. Concerning the meridional winds, we can notice very slight differences between the winter seasons. The equatorward component of the winter months gains magnitude with declining solar cycle whereas the northward component loses magnitude. For the other seasons, the magnitude of the meridional wind increases with declining solar cycle especially for spring and autumn months. We can clearly notice the presence of northward surges related to the MTM phenomenon present in all seasons but in a more pronounced way for autumn and spring months and in declining solar cycle. The thermosphere is in all seasons hotter in solar maximum and cooler in declining solar cycle. We should mention that the data have been averaged regardless of geomagnetic conditions. In the early evening hours, the seasonal slope of the temperature decrease seems to be similar for all years except for

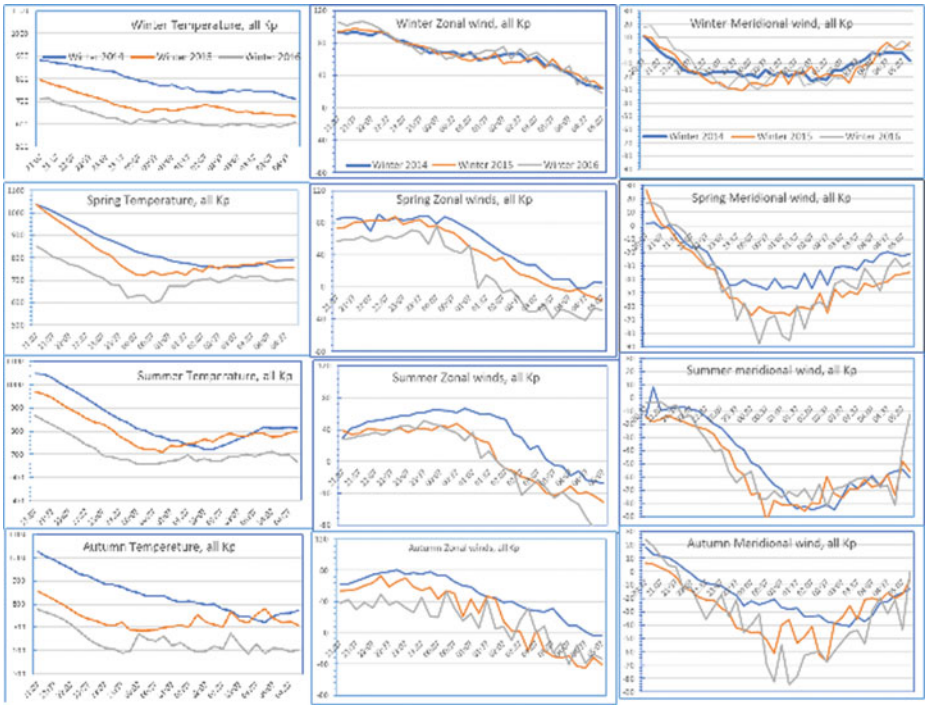

Figure 4. Variability with the solar cycle for the temperature data (left), the zonal winds (middle) and the meridional winds (right).

spring 2015. There seem to be important correlations between 2015 and 2016 seasonal temperature shape. The post-midnight heating of the thermosphere mostly related to the MTM phenomenon is more pronounced with declining solar cycle and in autumn months. The MTM phenomenon seem to occur predominantly in post-midnight hours. This is consistent with MTM observed phenomenon over many places (Meriwether *et al.* 2008, 2011).

5. Quiet and storm time variability

During geomagnetic storms, joule heating created by an increase of convective electric fields and auroral precipitation drives a global atmospheric change. The energy input drives wave surges that interact globally with the background wave mechanism (Buonsanto 1990).

The highly variable forcing sources cause disturbances to thermospheric winds which will further affect the global ionospheric dynamo (Blanc & Richmond, A. 1980). In disturbed geomagnetic conditions, thermospheric neutral winds exhibit large deviations from their quiet time climatological behavior resulting in large corresponding changes in the ionospheric plasma density, composition, temperature, and electrodynamics (Richmond & Matsushita 1975; Fuller-Rowell *et al.* 1994; Buonsanto 1990; Mendillo 2006; Meriwether *et al.* 2008; Emmert *et al.* 2004).

Through the FPI data we have noticed that in storm time, thermospheric winds depart from their habitual quiet time climatology in a variety of ways depending on the season, the magnitude of the storm, the dynamics of the storm energy release and the time of the storm. When the energy release is impulsive Traveling Atmospheric Disturbances (TADs)

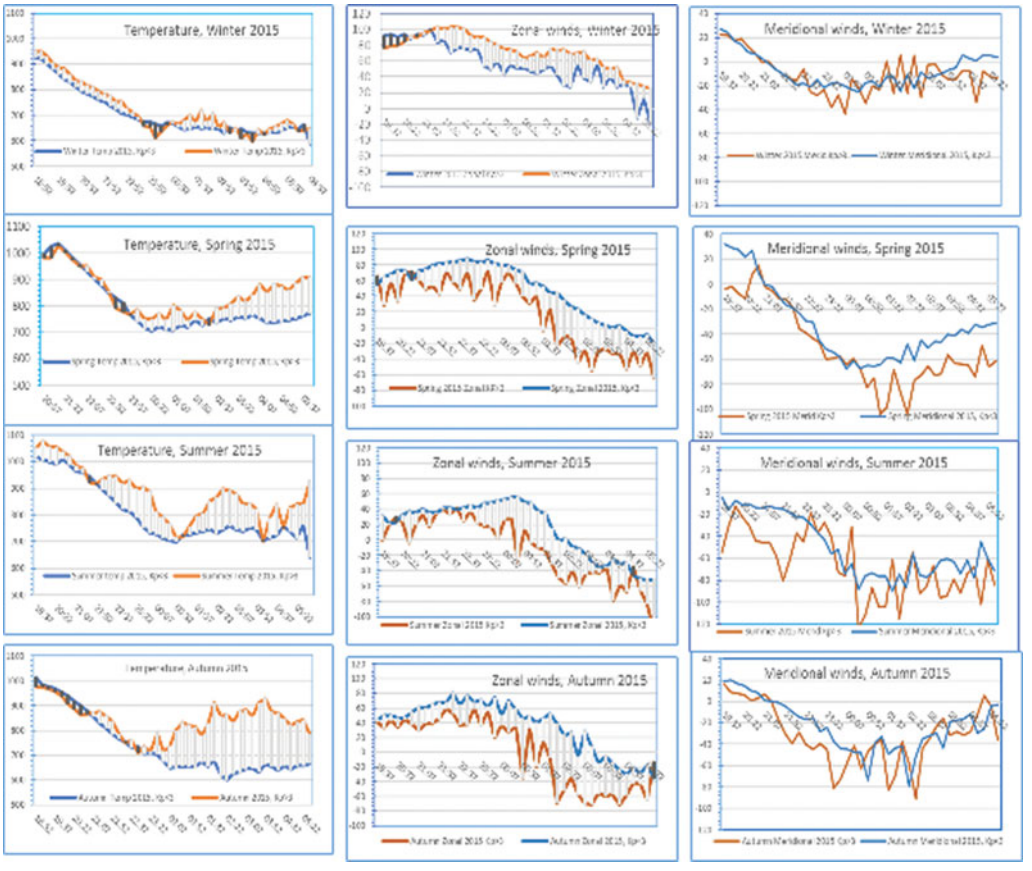

Figure 5. Seasonal effect of the storm. Quiet time data refer to data with 3 hours $K_p < 3$ and disturbed time data with 3 hours $K_p > 3$.

propagate from high to low latitudes and to the opposite hemisphere. A consequence of the TAD is the raise and fall of the ionospheric plasma along magnetic field lines creating Traveling Ionospheric Disturbances (TIDs). A storm induced Hadley cell is created flowing in opposite direction from quiet time one, with equatorward and westward winds. The variety of ways the thermospheric wind response to the storm depends on the extent reached by the storm induced Hadley cell.

Figure 5 illustrates the seasonal effect of the storm. The data have been separated into quiet-time data and geomagnetically disturbed-time data. The quiet time refer to data with 3-hour $K_p < 3$. The thermospheric data are related to the 2015 year. We must mention that the other years have the same trend as that of 2015. The averaged data reveals the general trends during storm time, but relevant information are exhibited from the study of each storm case separately. We can see in all seasons the equatorward storm surges and trans-equatorward surges in the meridional winds. The disturbed zonal winds, consisting of the storm winds minus the average quiet time winds, are westward. This result of westward and equatorward winds during the magnetic storm is consistent with previous results obtained with ground based Fabry-Perot interferometers (Makela & Miller 2011). Xiong *et al.* (2015) report that the disturbance zonal wind is mainly westward, and increases with magnetic activity and latitude. Emmert *et al.* (2004) reported westward and equator-ward night-time disturbed winds at midlatitude. Winter

time thermospheric heating is lower compared to other seasons with some oscillations subsequent to the quiet time temperature inflection point. The thermosphere seems to be heated in early evening hours. Winter storm meridional surges are very low compared to other seasons. Summer and autumn storm heating of the thermosphere is the highest. We can notice the presence of oscillations in the storm time summer shape of the temperature.

6. Conclusion

In this paper we have presented the thermospheric properties over Oukaimeden observatory, a typical mid-latitude site in the African continent. These properties consist of thermospheric winds and temperature measured with a Fabry-Perrot interferometer. We have illustrated the seasonal behavior of these data and the dependence on solar cycle. We have also illustrated the seasonal response of the thermosphere to the storm and how the storm time data depart from the quiet time trend.

References

Akmaev, R. A., Wu, F., Fuller-Rowell, T. J., Wang, H. & Iredell, M. D. 2010, *J. Geophys. Res.*, 115, A08326

Blanc, M. & Richmond, A. 1980, *Journal of Geophysical Research: Space Physics*, 85, 1669-1686.

Buonsanto, M. 1990, *Journal of Atmospheric and Terrestrial Physic*s, 52, 223-240.

Chapman, S. & Lindzen, R. S. 1970, Atmospheric tides: thermal and gravitational. Dordrecht : Reidel

Drob, D. P., Emmert, J. T., Meriwether, J. W., Makela, J. J., Doornbos, E., Conde, M., Hernandez, G., Noto, J., Zawdie, K. A., McDonald, S. E., Huba, J. D. & Klenzing, J. H. 2015, *Earth and Space Science*, 2, 301-319

Emmert, J., Picone, J., Lean, J. & Knowles, S. 2004, *Journal of Geophysical Research: Space Physics*, 109 (A2)

Fisher, D. J., Makela, J. J., Meriwether, J. W., Buriti, R. A., Benkhaldoun, Z., Kaab, M. & Lagheryeb, A. 2015, *Journal of Geophysical Research A: Space Physics*, 120, 6679-6693

Forbes, J. M. & Garrett, H. B. 1979, *Rev. Geophys.*, 17, 1951-1981

Fuller-Rowell, T., Codrescu, M., Moffett, R. & Quegan, S. 1994 *Journal of Geophysical Research: Space Physics*, 99, 3893-3914

Hagan, M. E & Forbes, J. M. 2002, *Journal of Geophysical Research*, 107, D24, 4754

Harding, B. J., Gehrels, T. W. & Makela, J. J. 2014, *Appl. Opt.*, 53, 666-673

Harding, B. J, Midlatitude thermospheric wind and temperature: Networked Fabry-Perot interferometer observations and radiative transfer modeling, (2017), Thesis Ph.D degree.

Kaab, M., Benkhaldoun, Z., Fisher, D. J., Harding, B., Bounhir, A., Makela, J. J., Laghriyeb, A., Malki, K., Daassou, A. & Lazrek. M. 2017, *Annales Geophysicae*, 35, 161-170

Link, R. & Cogger, L. 1988, *J. Geophys. Res.-Space*, 93, 9883-9892

Makela, J. J. & Miller, E. S. 2011, *Aeronomy of the Earth's Atmosphere and Ionosphere* , vol 2, 239-249

Meriwether, J., Faivre, M., Fesen, C., Sherwood, P. & Veliz,O. 2008, *Annales Geophysicae*, 26, 447-466

Meriwether, J. W., Makela, J. J., Huang, Y., Fisher, D. J., Buriti, R. A., Medeiros, A. F. & Takahashi, H. 2011, *Journal of Geophysical Research*, 116 , A04322

Mendillo, M. 2006, *Reviews of Geophysics*, 44, 2006

Richmond, A. & Matsushita, S. 1975, *Journal of Geophysical Research*, 80, 2839-2850

Smith, C. W., LHeureux, J., Ness, N. F., Acuña, M. H., Burlaga, L. F. & Scheifele, J. 1998, *ISpace Science Reviews*, 86, 613-632

Xiong, C., Lühr, H. & Fejer, B. G. 2015, *Journal of Geophysical Research (Space Physics)*, 120, 5137-5150